Bull. Mater. Sci., Vol. 34, No. 7, December 2011, pp. 1331–1338. © Indian Academy of Sciences.

Synthesis of one-dimensional N-doped Ga_2O_3 nanostructures: different morphologies and different mechanisms

S C VANITHAKUMARI and K K NANDA*
Materials Research Centre, Indian Institute of Science, Bangalore 560 012, India

MS received 30 November 2009

Abstract. **N-doped monoclinic Ga_2O_3 nanostructures of different morphologies have been synthesized by heating Ga metal in ambient air at 1150°C to 1350°C for 1 to 5 h duration. Neither catalyst nor any gas flow has been used for the synthesis of N-doped Ga_2O_3 nanostructures. The morphology was controlled by monitoring the curvature of the Ga droplet. Plausible growth mechanisms are discussed to explain the different morphology of the nanostructures. Elemental mapping by electron energy loss spectroscopy of the nanostructures indicate uniform distribution of Ga, O and N. It is interesting to note that we have used neither nitride source nor any gas flow but the synthesis was carried out in ambient air. We believe that ambient nitrogen acts as the source of nitrogen. Unintentional nitrogen doping of the Ga_2O_3 nanostructures is a straightforward method and such nanostructures could be promising candidates for white light emission.**

Keywords. **Ga_2O_3 nanostructures; nitrogen doping; white light emission; growth mechanism.**

1. Introduction

White light emission is usually generated either by coating a yellow phosphor on a blue light emitting diode (LED) made of InGaN, or by mixing three primary colors (red, green and blue) by using a multilayer structure or doping an active host material with several fluorescent dyes, or composites. Recently, white light emission from nanostructures has become the research of general interest as a motive to replace the conventional device of white light emission (Bol *et al* 2001; Cheah *et al* 2002; Achermann *et al* 2004; Bowers *et al* 2005; Chen *et al* 2005; Lu *et al* 2005; Sui *et al* 2005; Ali *et al* 2007; Sapra *et al* 2007). These systems are based on ZnO (Sui *et al* 2005), CdSe (Bowers *et al* 2005) and a mixture of different size/composition nanocrystals (Achermann *et al* 2004; Ali *et al* 2007), ZnS : Pb (Bol *et al* 2001), ZnS incorporated in porous silicon (Cheah *et al* 2002), ZnSe (Chen *et al* 2005), Mn-doped ZnS (Lu *et al* 2005) and CdSe core with three shells comprised of ZnS/CdSe/ZnS (Sapra *et al* 2007). CdSe being a semiconductor with a bulk band gap of 1·74 eV, the band gap of CdSe nanocrystals depends significantly on the crystal size (Nanda *et al* 2001). This suggests that specific size of the crystal is required to imitate white light emission as observed by Bowers *et al* (2005). On the other hand, wide-band-gap semiconductors such as Ga_2O_3, ZnO, ZnS, In_2O_3, etc depend very weakly on the size of the crystals. Therefore, wide-band-gap materials are more appropriate for this kind of applications.

Ga_2O_3 is a wide-band-gap (4·9 eV) semiconductor that has been used as a light emitter (Ogita *et al* 1999; Li *et al* 2000). Visible blue-green emission is reported for Ga_2O_3 nanoparticles (Lam *et al* 2004; Chen and Tang 2007), while nanorods emit UV-blue light extended to green region (Liang *et al* 2001; Chang and Wu 2004; Zhang *et al* 2004) when irradiated with an UV light of energy greater than the band gap of Ga_2O_3. It may be noted here that a red emission along with blue-green emission is required for the generation of white light. Red emission has been reported for Ga_2O_3 nanostructures doped with N, Cr or Eu (Song *et al* 2004; Kim and Kim 2005; Nogales *et al* 2007a, b; 2009). Doping of Cr or Eu can be achieved in two ways (Nogales *et al* 2007a, b; 2009): (i) by post annealing of the Ga_2O_3 samples in the presence of Cr_2O_3/Eu_2O_3 powders and (ii) thermal evapouration of the mixture of Ga_2O_3 and Cr_2O_3/Eu_2O_3 powders compacted into pellets. Doping of Ga_2O_3 nanostructures involve either post annealing or a lengthy procedure. On the other hand, nitrogen doping can be achieved either by annealing Ga_2O_3 in N_2/NH_3 or by using a GaN source (Song *et al* 2004; Kim and Kim 2005). Recently, we have reported the one-step growth of N-doped one-dimensional (1D) Ga_2O_3 nanorods and their light emitting behaviour (Nogales *et al* 2009).

Here, we report the synthesis of N-doped Ga_2O_3 nanostructures of different morphologies by heating molten Ga in air ambient. By exploring the curvature of molten Ga, different morphology such as nanorods, nanobelts and nanoneedles are obtained. Neither catalyst nor any

*Author for correspondence (nanda@mrc.iisc.ernet.in)

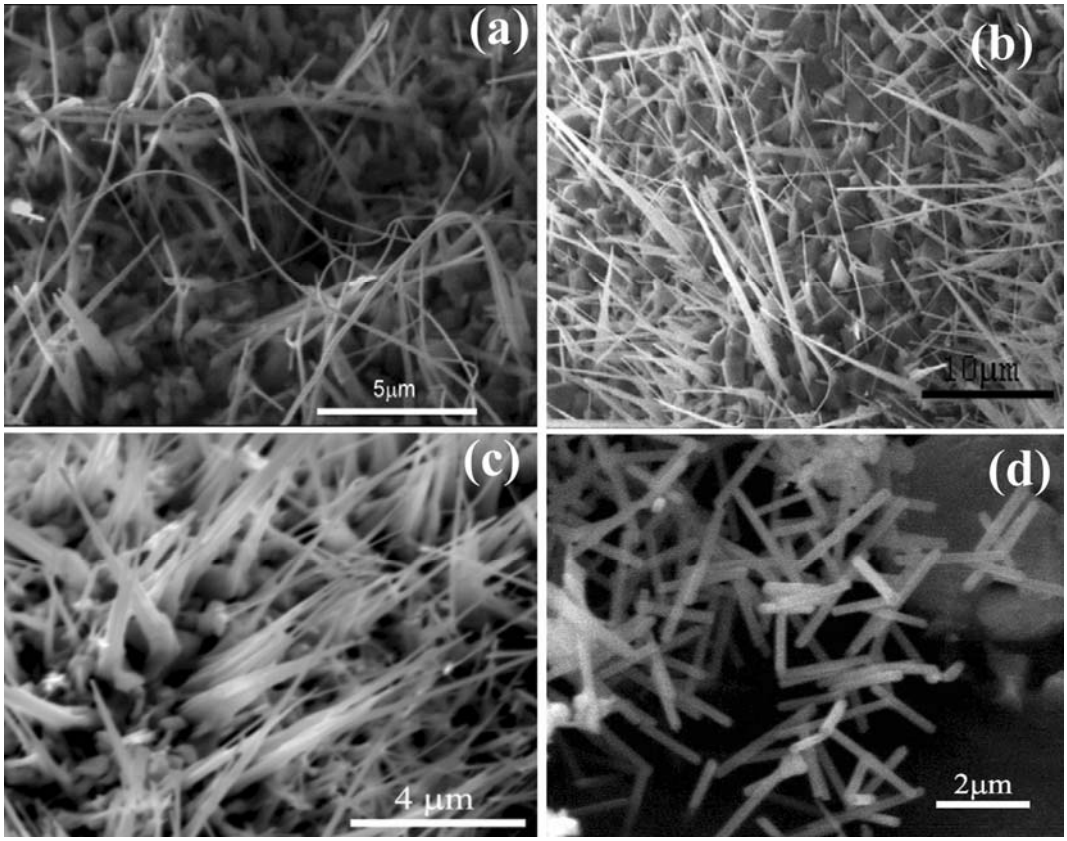

Figure 1. SEM images of (**a**) Ga_2O_3 nanobelts obtained by heating the molten Ga painted on c-sapphire substrate; 1250°C, 3 h; (**b**) Ga_2O_3 nanoneedles obtained by heating the molten Ga painted on quartz substrate; 1250°C, 3 h; (**c**) Ga_2O_3 nanorods obtained by heating the Ga droplet placed on a silicon substrate; 1250°C, 3 h and (**d**) Ga_2O_3 nanorods obtained by heating the Ga droplet placed in a quartz boat; 1300°C, 4 h.

gas flow is required for the synthesis of N-doped Ga_2O_3 nanostructures. We have ensured the presence of N along with Ga and O in these nanostructures and they are uniformly distributed over the nanorods. The probable growth mechanisms for the different morphologies of the nanostructures are discussed. We also report the optical properties of N-doped Ga_2O_3 nanostructures.

2. Experimental

Molten Ga (99·999% purity; Sigma Aldrich) was taken on a silicon substrate, quartz boat, and a thin layer of molten Ga was painted on sapphire, quartz substrates and heated in a horizontal tube furnace in air ambient. The experiment was carried out at temperatures ranging from 1150°C to 1350°C for a duration of 1 to 5 h. The final products were white in colour. The morphology of the nanostructures was examined by scanning electron microscopy (SEM) and transmission electron microscopy (TEM). The phase and the crystallinity of the samples were ascertained by X-ray diffraction (XRD) and TEM coupled with energy dispersive spectroscopy (EDS). The optical quality of the nanorods was examined by Raman spectroscopy with a 514·5 nm wavelength Ar ion laser. The compositions of the samples were examined by X-ray photoelectron spectroscopy (XPS). The elemental mapping of the nanorods were obtained by electron energy-loss spectroscopy (EELS) coupled with TEM.

3. Results and discussion

Figures 1a and b show the scanning electron microscope (SEM) images of molten Ga painted on sapphire and quartz substrates that show the formation of nanobelts (length ~ 10–20 μm and thickness ~ 50 nm) and nanoneedles (length ~ 10–20 μm and diameter ~ 100 nm), respectively. The temperature is maintained at 1250°C for 3 h in the case of molten Ga painted on sapphire and quartz substrates. Figure 1c shows the SEM image of the nanorods synthesized on a silicon substrate. In this case molten Ga droplet is placed on Si substrate and heated at 1250°C for 3 h. It is worthy to point out here that when Ga is placed on a Si substrate a part of the substrate is consumed, leaving a hole. This clearly confirms the fact

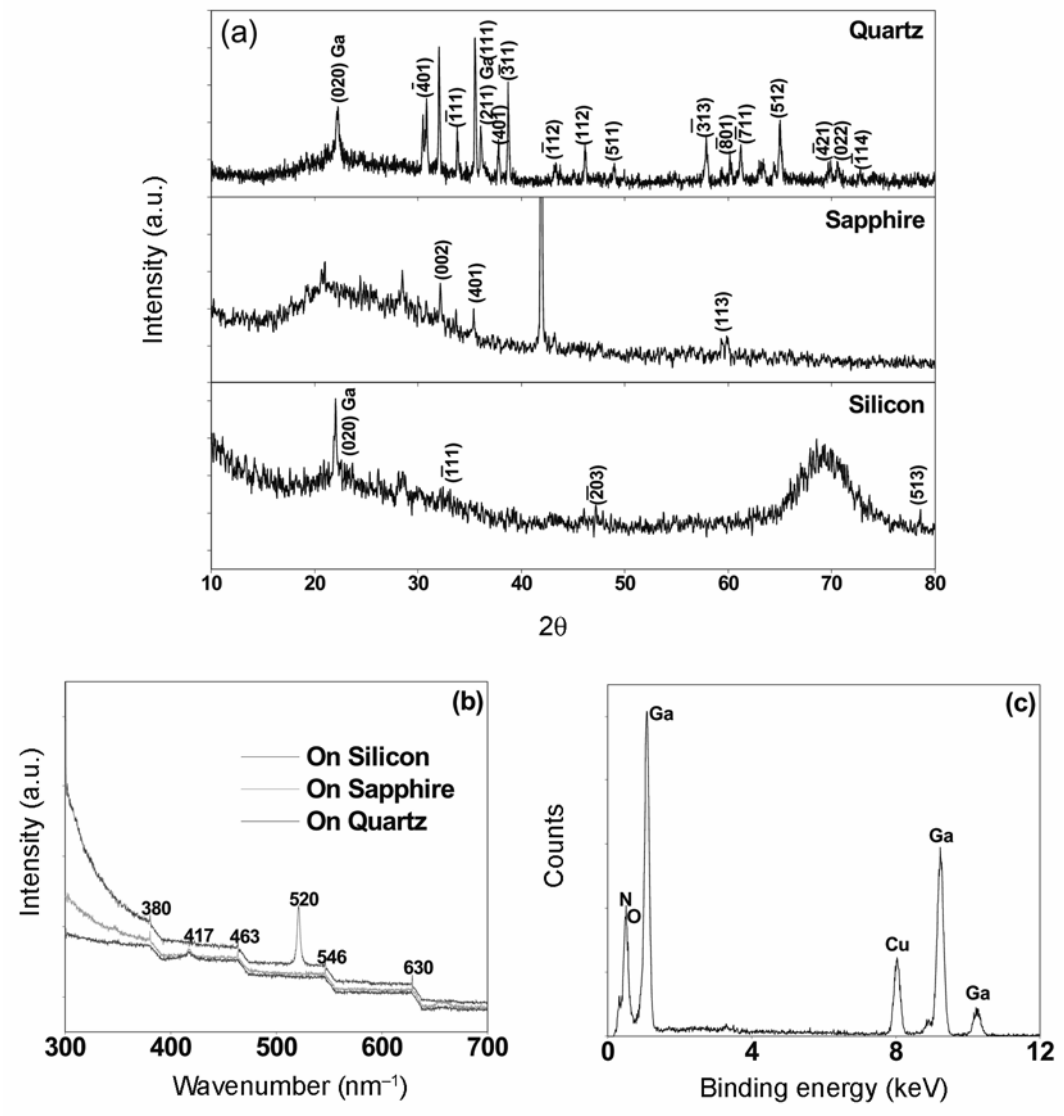

Figure 2. (**a**) XRD pattern, (**b**) Raman spectra and (**c**) EDS spectrum of the Ga_2O_3 nanostructures.

that Ga dissolves silicon from the substrate (Heck and Broder 1953). Figure 1d shows the SEM image of the nanorods when molten Ga is heated in a quartz boat at 1300°C for 4 h. The average diameter and length of the nanorods are 100 nm and 2 μm, respectively.

Figure 2a shows the X-ray diffraction (XRD) patterns of nanostructures synthesized on silicon, sapphire and quartz substrates. The position of the XRD peaks shows a good agreement with the monoclinic phase of Ga_2O_3. The lattice parameters are evaluated to be $a = 12{\cdot}277$ Å; $b = 3{\cdot}046$ Å; $c = 5{\cdot}8$ Å and $\beta = 103{\cdot}70°$ and are comparable with JCPDS file. A few peaks corresponding to the residual Ga in the sample are also observed. Raman spectra for the nanostructures synthesized on silicon, sapphire and quartz substrates are shown in figure 2b. The peaks at 380, 417, 463, 520, 546 and 630 cm^{-1} in the spectrum are in good agreement with the results reported in the literature for Ga_2O_3 (Choi *et al* 2000). An energy dispersive (EDS) spectrum of rods on a Cu grid is shown in figure 2c. It may be noted that a trace of N is present in the samples along with Ga and O, whereas the Cu peak is from Cu grid.

Figure 3a shows the TEM image, high-resolution TEM (HRTEM) and fast Fourier transform (FFT) patterns of a nanorod synthesized from molten Ga placed on a silicon substrate and heated at 1250°C for 3 h. The average diameter of the rod varies from 280 nm at the base to 260 nm at the tip. Similarly, the bright field images, HRTEM and diffraction patterns of the nanostructures synthesized on sapphire and quartz substrates are shown in figures 3b and c, respectively. The growth directions of the nanostructures are shown by arrows. It may be noted that the growth direction is either [001] or [200] for the nanostructures synthesized on silicon, sapphire and

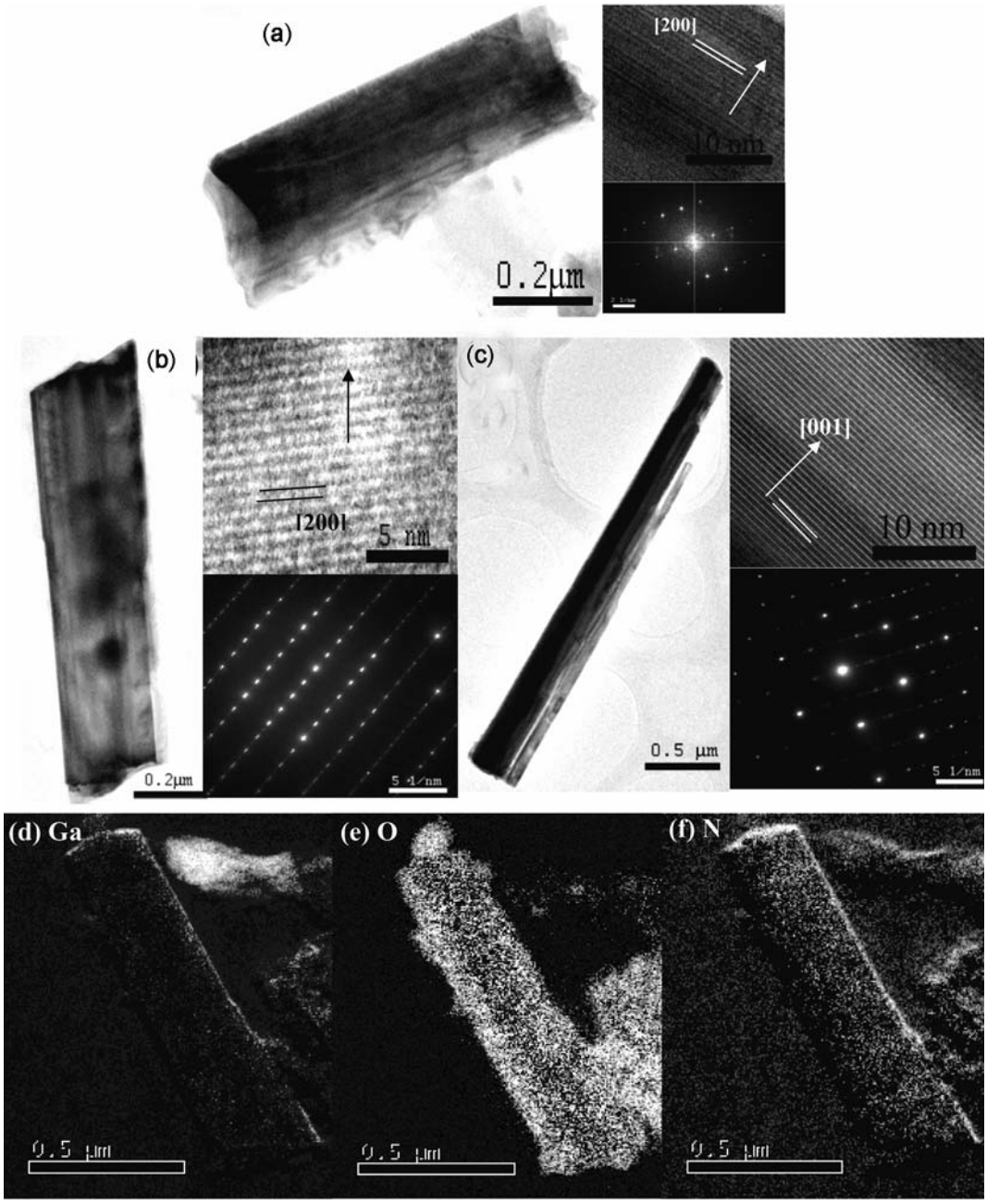

Figure 3. TEM images, HRTEM and corresponding diffraction pattern of Ga_2O_3 nanostructures obtained by heating the Ga droplet placed on (**a**) silicon, (**b**) sapphire and (**c**) quartz substrates. (**d–f**) Elemental mapping of a single Ga_2O_3 nanorod synthesized on a silicon substrate by TEM coupled with EELS.

quartz substrates. The corresponding selected area electron diffraction (SAED) patterns are indexed to monoclinic phase of Ga_2O_3. From the XRD and HRTEM investigation, it may be concluded that the Ga_2O_3 nanostructures synthesized on different substrates are single crystalline. Figures 3d–f are the elemental mapping of a single Ga_2O_3 nanorod by TEM coupled with electron energy loss spectroscopy (EELS) that indicates almost uniform distributions of Ga, N and O in the nanorods.

Figures 4a–e show the X-ray photoelectron (XPS) spectra of C 1*s*, O 1*s*, Ga 2*p* and N 1*s* for the Ga_2O_3 nanostructures obtained by heating the Ga droplet placed on silicon (represented by black squares) and sapphire (represented by red squares) substrates at 1250°C for 3 h. The insets in graphs (4a–c) represent the deconvoluted spectra of C 1*s*, O 1*s* and Ga 2*p* in the Ga_2O_3 nanostructures synthesized on a silicon substrate. In the case of C 1*s* from the Ga_2O_3 nanostructures on silicon, there are two peaks. The peak around 284·8 eV corresponds to the elemental

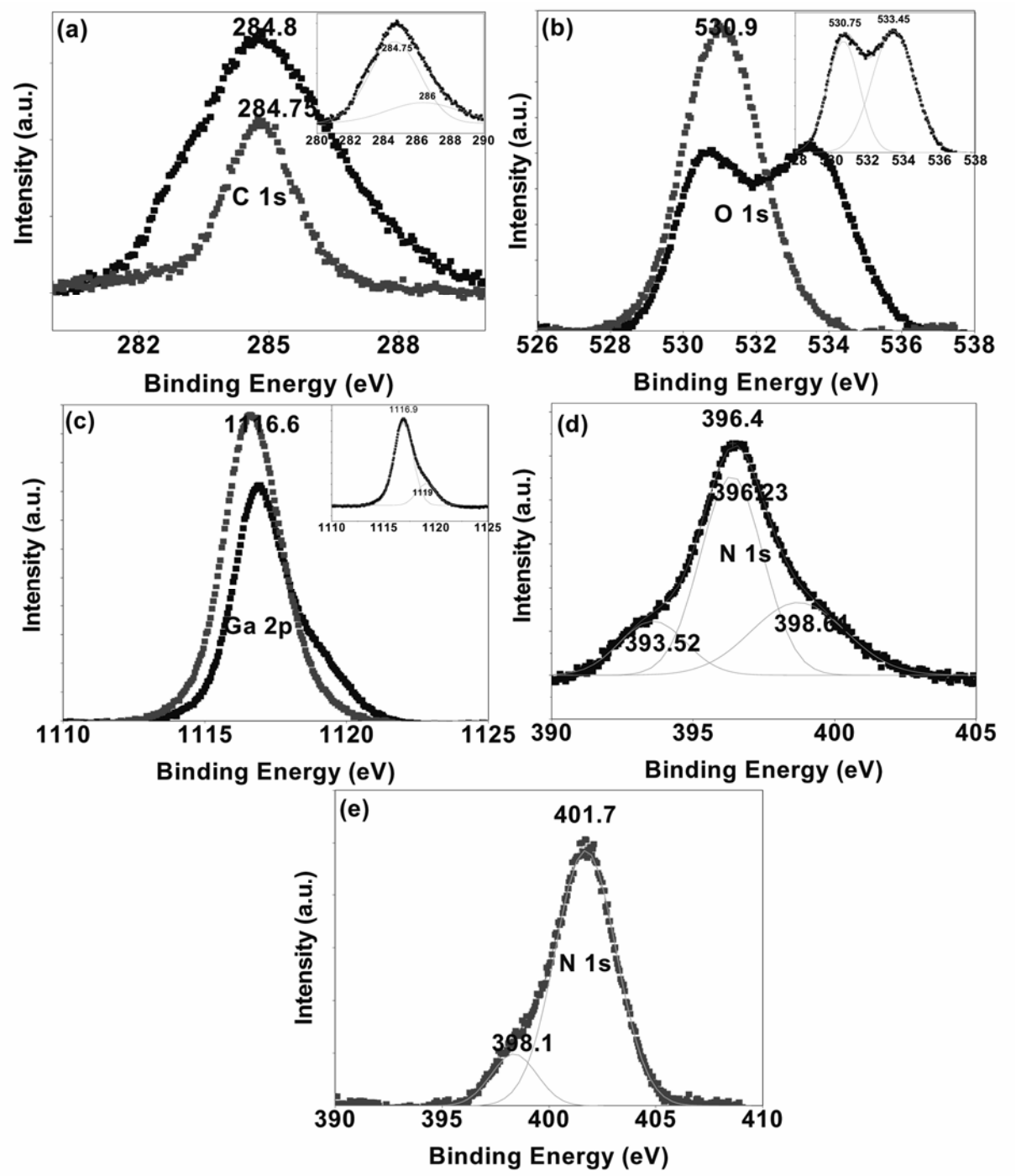

Figure 4. XPS spectra for Ga_2O_3 nanostructures obtained by heating the Ga droplet placed on silicon (represented by black squares) and sapphire (represented by red squares) substrates at 1250°C for 3 h. The insets in graphs (**a–c**) represent the deconvoluted spectra of C 1*s*, O 1*s* and Ga 2*p* in the Ga_2O_3 nanostructures synthesized on a silicon substrate. The graphs (**d** and **e**) represent the deconvoluted N 1*s* spectra of silicon and sapphire substrates, respectively.

carbon as inferred from http://srdata.nist.gov/xps, and the peak at 285·7 eV is due to the nitrogen incorporation in the sample (Bouchet-Fabre *et al* 2005). There is a doublet peak in the O 1*s* spectrum for silicon, whereas there is no doublet in the case of sapphire. The positions of different peaks are given in tabular form (table 1). The O 1*s* peaks around ~ 531 eV in both substrates is due to the presence of oxygen species in Ga_2O_3 (http://srdata.nist.gov/xps). The second O 1*s* peak in the silicon substrate at 533·45 eV corresponds to SiO_2 (http://srdata.nist.

Table 1. XPS characterization of nitrogen doped Ga_2O_3 nanorods.

Substrate	Elements	Peak position (eV)	Peak identification
Silicon	C 1s	284·8	Elemental carbon
		285.7	Nitrogen incorporation
	O 1*s*	530·75	Oxygen species in Ga_2O_3
		533·45	SiO_2
	Ga 2*p*	1116·9	Ga–N bonding/Ga–O bonding
		1119	Ga–O bonding
	N 1*s*	393·7	A compound of C, H, O, N
		396·48	N-doped Ga_2O_3
		398·86	N-doped Ga_2O_3
Sapphire	C 1*s*	284·75	Elemental carbon
	O 1*s*	530·9	Oxygen species in Ga_2O_3
	Ga 2*p*	1116·95	Ga–N bonding/Ga–O bonding
	N 1*s*	398·56	N-doped Ga_2O_3
		402	A form of NO

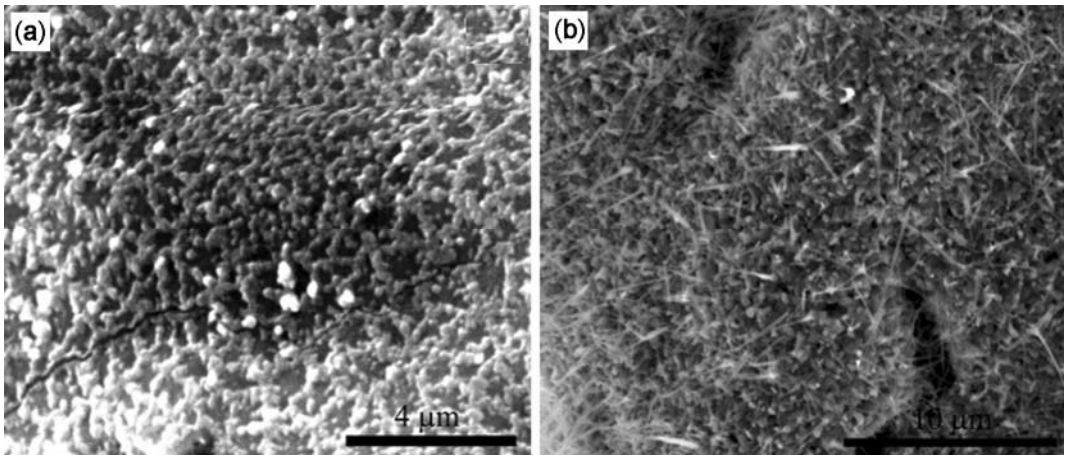

Figure 5. SEM images of molten Ga painted on c-sapphire substrate and heated in ambient at (**a**) 600°C; 30 min and (**b**) 950°C; 3 h.

gov/xps). The N 1*s* spectrum shown in figure 4e for silicon substrate is deconvoluted into three peaks, the peak at 393·7 eV is due to the presence of a compound of C, N, O and H ((http://srdata.nist.gov/xps). Note that there is a doublet in the C 1*s* spectrum. The peaks at 396 and 398 eV are attributed to N-doped Ga_2O_3 with different N concentrations (Song *et al* 2004). The Ga 2*p* spectrum for silicon substrate is also deconvoluted to two peaks. In both the substrates, Ga 2*p* peak at 1116·9 eV is common and corresponds to the Ga–O bonding in Ga_2O_3 (http://srdata.nist.gov/xps). The second Ga 2*p* peak at 1119 eV and the N 1*s* peak at 396·48 eV suggest two different chemical environments of Ga_2O_3, i.e. some regions of the sample are more N-rich than others. But this effect is not prominent while characterizing the sample with EELS, which shows an almost uniform distribution of Ga, O and N. The N 1*s* spectrum of sapphire substrate shown in figure 4e is deconvoluted into two peaks, the binding energy at 398·56 eV corresponds to N of N-doped Ga_2O_3 (Song *et al* 2004), while the energy at 402 eV corresponds to nitrogen in C_3N_4 (Kusunoki *et al* 2001) or due to a form of NO (Bouchet-Fabre *et al* 2004).

The growth mechanism of the Ga_2O_3 nanorods produced by heating Ga droplet in quartz boat is discussed by Vanithakumari and Nanda (2009). However, the morphologies are different for the nanostructures synthesized on silicon, sapphire and quartz substrates and the growth mechanisms are expected to be different. SEM images of the molten Ga painted on c-sapphire substrate heated to 600°C for 30 min and 950°C for 3 h are shown in figures 5a and b. In figure 5a, the formation of island-like base could be seen. When the substrate is heated at higher temperature, the island-like base serves as the growth centre for the nanobelt formation as shown in figure 5b. SEM images of nanobelts obtained by heating the molten Ga painted on c-sapphire substrate at two different temperatures but for the same time duration are shown in figures 6a and b. It is evident that the density of nano-

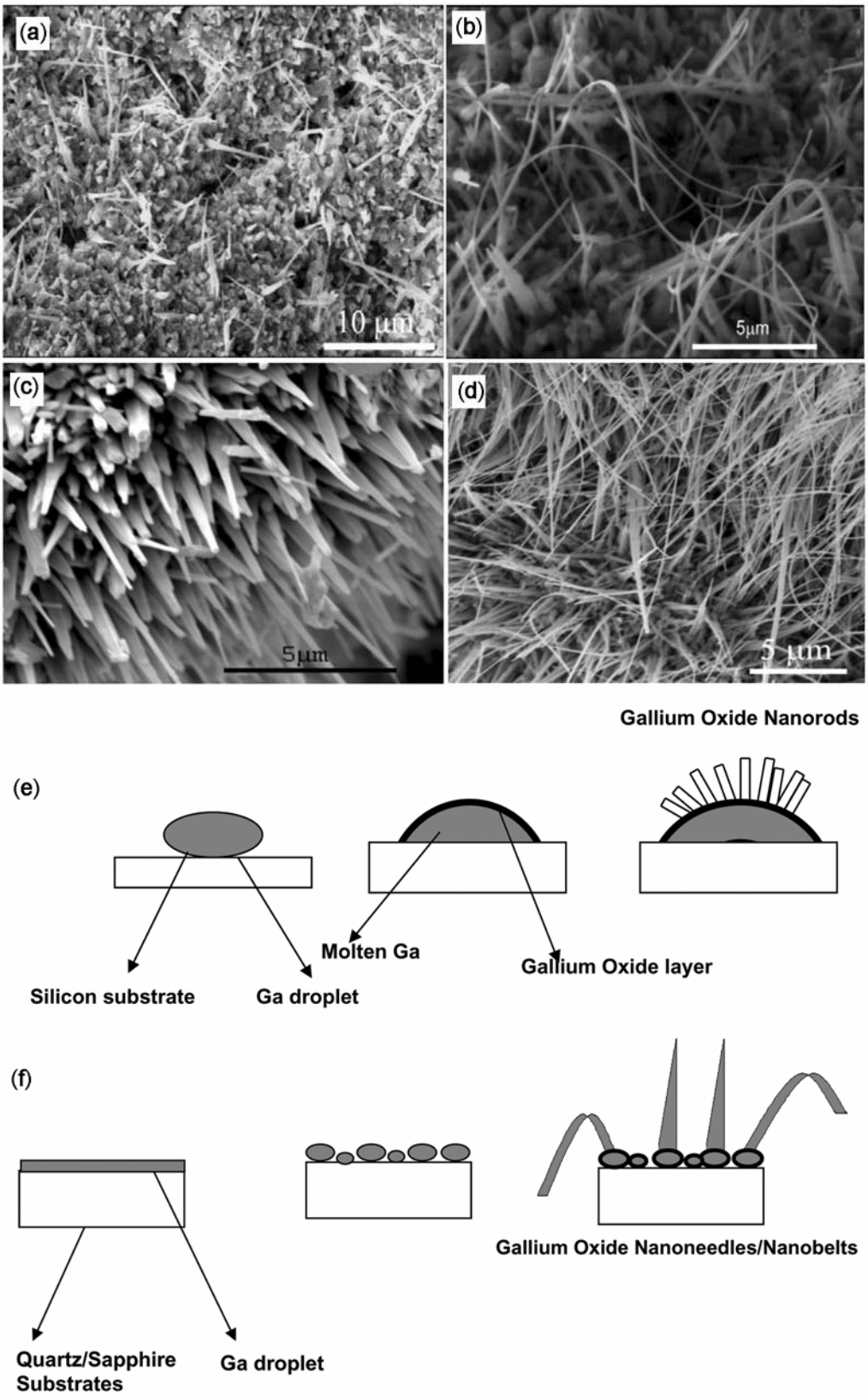

Figure 6. SEM images of Ga_2O_3 nanobelts obtained by heating the molten Ga painted on c-sapphire substrate: (**a**) 1150°C; 3 h, (**b**) 1250°C; 3 h. Ga_2O_3 nanorods obtained by heating the Ga droplet placed on a silicon substrate: (**c**) 1150°C; 3 h and (**d**) 1150°C; 5 h. Schematic of growth mechanism of Ga_2O_3 (**e**) nanorods synthesized from molten Ga placed on a silicon substrate and (**f**) nanobelts/nanoneedles synthesized from molten Ga painted on sapphire and quartz substrates.

structures increases with temperature. Shown in figures 6c and d are the SEM images of nanorods obtained by heating the Ga droplet placed on a silicon substrate at the same temperature but for different time duration. The length of the nanorods increases with synthesis time. Overall, density of the nanostructures is controlled by temperature, while duration of heat treatment controls the aspect ratio of the nanostructures.

When the temperature is raised from room temperature to the desired preparation temperature, surface of the molten Ga oxidizes while the core remains unoxidized. With these key points, we suggest an oxide-assisted base growth mechanism for the Ga_2O_3 nanostructures. As the vapour pressure of Ga is very large as compared to Ga_2O_3 (Samsonov 1982) and the lattice constants and the thermal expansion of Ga_2O_3 are different from Ga, the oxide layer will be under strain and cracks in the outer Ga_2O_3 layer are expected. As the vapour pressure of Ga at the synthesis temperature is high, Ga vapours escape through the cracks where they react with atmospheric oxygen and nitrogen to form N-doped Ga_2O_3. This process continues to form 1D nanostructures.

Now, we shed some light on the different morphology of the nanostructures. It is apparent from figures 1, 5 and 6 that the nanobelts and nanoneedles on sapphire and quartz substrates have island-like base and the size of the island is few hundred nm. A large Ga droplet of few mm diameter is placed in case of silicon substrate, whereas a thin layer of molten Ga is painted on sapphire and quartz substrates. The thin layer of Ga on substrates breaks into smaller droplets as evident from figure 5. Key issue associated with different morphology is believed to be due to curvature effect. The surface of Ga droplet on silicon is expected to be flat and nanorods are obtained for Ga droplet placed on silicon substrate (figures 1c and 6c). The schematic of the growth mechanisms on silicon and sapphire/quartz are shown in figures 6e and f, respectively. When the droplets are small, the formation of crack favours the formation of belt-like 1D nanostructures, while uniform rods are formed on the surface of large droplet. The curvature of the starting material and the vapour pressure of the source material at the growth temperature are the key factors that control the morphology and the length-to-diameter ratio of the Ga_2O_3 nanostructures.

4. Conclusions

Single-crystalline monoclinic phase of nitrogen-doped Ga_2O_3 nanorods, nanobelts and nanoneedles were synthesized by heating molten Ga in air ambient. The morphology was controlled by monitoring the curvature of the Ga droplet. Possible growth processes of different morphology have been proposed. The unintentional nitrogen doping of the Ga_2O_3 nanostructures need further investigation and such nanostructures could be promising candidates for white light emission.

References

Achermann M, Petruska M A, Kos S, Smith D L, Koleske D D and Klimov V I 2004 *Nature* **429** 642

Ali M, Chattopadhyay S, Nag A, Kumar A, Sapra S, Chakraborty S and Sarma D D 2007 *Nanotechnology* **18** 075401

Bol A A and Meijerink A 2001 *Phys. Chem. Chem. Phys.* **3** 2105

Bouchet-Fabre B, Godet C, Lacerda M, Charvet S, Zellama K and Ballutaud D 2004 *J. Appl. Phys.* **95** 3427

Bouchet-Fabre B, Marino E, Lazar G, Zellama K, Clin M, Ballutaud D, Abel F and Godet C 2005 *Thin Solid Films* **482** 167

Bowers II M J, McBride J R and Rosenthal S J 2005 *J. Am. Chem. Soc.* **127** 15378

Chang K W and Wu J J 2004 *Adv. Mater.* **16** 545

Cheah K W, Xu L and Huang X 2002 *Nanotechnology* **13** 238

Chen H S, Wang S J J, Lo C J and Chi J Y 2005 *Appl. Phys. Lett.* **86** 131905

Chen T and Tang K 2007 *Appl. Phys. Lett.* **90** 053104

Choi Y C, Kim W S, Park Y S, Lee S M, Bae D J, Lee Y H, Park G S, Choi W B, Lee N S and Kim J M 2000 *Adv. Mater.* **12** 746

Heck P H and Broder J 1953 *Phys. Rev.* **90** 521

Kim H W and Kim N H 2005 *Appl. Phys.* **A80** 537

Kusunoki I, Sakai M, Igari Y, Ishidzuka S, Takami T, Takaoka T, Nishitani-Gamo M and Ando T 2001 *Surf. Sci.* **492** 315

Lam H M, Hong M H, Yuan S and Chong T C 2004 *Appl. Phys.* **A79** 2099

Li Z, De Groot C and Moodera J H 2000 *Appl. Phys. Lett.* **77** 3630

Liang C H, Meng G W, Wang G Z, Wang Y W, Zhang L D and Zhang S 2001 *Appl. Phys. Lett.* **78** 3202

Lu H Y, Chu S Y and Tan S S 2005 *Jpn. J. Appl. Phys.* **44** 5282

Nanda K K, Kruis F E and Fissan H 2001 *NanoLett.* **1** 605

Nogales E, Méndez B, Piqueras J and García J Á 2009 *Nanotechnology* **20** 115201

Nogales E, García J Á, Méndez B and Piqueras J 2007a *Appl. Phys. Lett.* **91** 133108

Nogales E, García J Á, Méndez B and Piqueras J 2007b *J. Appl. Phys.* **101** 033517

Ogita M, Saika N, Nakanishi Y and Hatanaka Y 1999 *App. Sur. Sci.* **142** 188

Samsonov G V 1982 *The oxide handbook* (London: Plenum)

Sapra S, Mayilo S, Klar T A, Rogach A L and Feldmann J 2007 *Adv. Mater.* **19** 569

Song Y P, Zhang H Z, Lin C, Zhu Y W, Li G H, Yang F H and Yu D P 2004 *Phys. Rev.* **B69** 075304

Sui X M, Shao C L and Liu Y C 2005 *Appl. Phys. Lett.* **87** 113115

Vanithakumari S C and Nanda K K 2009 *Adv. Mater.* **21** 3581

Zhang J, Jiang F and Zhang L 2004 *Phys. Lett.* **A322** 363